



Gazi University

Journal of Science

PART A: ENGINEERING AND INNOVATION

<http://dergipark.org.tr/guj.1345002>

Effect of Annealing and Doping Process of the $Zn_{1-x}Ti_xO$ Films

Tuğba ÇORLU^{1,2} Sezen TEKİN^{3*} Irmak KARADUMAN ER³ Selim ACAR²

¹Suleyman Demirel University, Innovative Technologies Application and Research Center, Isparta, Türkiye

²Gazi University, Faculty of Science, Department of Physics, Ankara, Türkiye

³Çankırı Karatekin University, Eldivan Medical Services Vocational School, Department of Medical Services and Techniques, Çankırı, Türkiye

| Keywords | Abstract |
|--|---|
| Ti-doped ZnO SILAR Annealing Characterization | In this study, undoped and Ti-doped ZnO thin films grown by SILAR (Successive Ionic Layer Adsorption and Reaction) method were investigated using XRD, SEM, linear absorbance and electrical characterization. The effect of doping ratio was determined changing Ti ratios from 0.05 to 0.20. In addition, the films with the same additive ratio were annealed at 300°C for 15 minutes in nitrogen environment. Thus, the effects of both annealing and doping ratio on the thin films produced were examined in detail. When the current-voltage graphs are examined, it is observed that there is a decrease in the resistance values with doping. The best additive effect was observed for Zn _{0.90} Ti _{0.10} O film and the structures formed after this additive ratio returned to their initial morphology. |

Cite

Çorlu, T., Tekin, S., Karaduman Er, I., & Acar, S. (2023). Effect of Annealing and Doping Process of the $Zn_{1-x}Ti_xO$ Films. *GU J Sci, Part A, 10(3)*, 341-352. doi:10.54287/guj.1345002

| Author ID (ORCID Number) | Article Process |
|--------------------------|-----------------------------------|
| 0000-0001-5828-207X | Tuğba ÇORLU |
| 0000-0002-6599-9631 | Sezen TEKİN |
| 0000-0003-3786-3865 | Irmak KARADUMAN ER |
| 0000-0003-4014-7800 | Selim ACAR |
| | Submission Date 17.08.2023 |
| | Revision Date 29.08.2023 |
| | Accepted Date 18.09.2023 |
| | Published Date 27.09.2023 |

1. INTRODUCTION

Many studies have been carried out and model systems have been developed to improve the previously known properties of basic physical and chemical properties related to thin film performance and structure in various applications and to increase the progress in this field. The combined results of all these emerging experimental and theoretical investigations form the basis for the development of new thin film systems and shaping their structure and performance.

Thin films must have appropriate thickness, information and characteristic properties in order to exhibit the expected functions. For this purpose, the production studies of higher quality thin films are carried out trying different deposition methods and production on different substrate materials. Different methods are used to control the properties of thin films. One of these methods is the placement of impurity atoms to the structure. The impurity atoms must be smaller or equal in diameter than the host ions, and at the same time, the doping atoms must have an extra electron compared to these ions. This situation is not only one of the most important conditions for doping, but also means fewer crystal defects, since in such a case the lattice tension is less and it also leads to high electrochemical stability.

Titanium (Ti) was chosen as the impurity for ZnO thin films in this study. It has partially filled d shells, and it can replace the ions of the host semiconductor, so that the titanium can easily settle into the structure. In addition, Ti fully complies with the conditions mentioned below. Both ionic and covalent diameters (0.068 nm and 0.136 nm) are closest to those of zinc (0.072 nm and 0.131 nm). In this way, any structural changes or microstructural defects cannot be observed after settling impurity into the structure. Titanium doping has many effects on the properties of zinc oxide. One of them is that the extra free electrons from Ti reduce the electrical

resistance and increase the conductivity (Hsu et al., 2016). The fact that Ti provides two extra free electrons also ensures that doping at a lower concentration is sufficient to achieve a high degree of conductivity, which is costly (Hsu et al., 2016). Another plus of this situation is that due to the improvement of the electrical properties, the response of the structure also increases, and the decrease in the resistance causes more sensor response in general (Shewale & Yu, 2016). In addition, the addition of Ti impurity atoms can reduce the crystal size of the samples and improve the specific surface areas of the samples concerned (Darmadi et al., 2020). Another benefit of Ti doping is that it increases the device capacitance and reduces the reactivity to humidity in the environment. Being a chemically stable material makes it suitable for biochemical detection (Lee et al., 2018). However, one of the most important points to be considered during doping is the amount of titanium to be used, because if the additive is too much, it may settle in the interatomic regions in the structure and the desired properties may not be achieved (Lee et al., 2018).

Various physical and chemical based methods are used to grow thin films. However, these physically-based methods require high costs and superior device performance. Chemical-based methods are more preferred because they are affordable, fast, environmentally friendly and can be found easily. There are some studies about the Ti-doped ZnO samples with different grown methods and investigate physical and chemical methods. Samuel et al. (2022) have predetermined pure and Ti-doped ZnO samples with the hydrazine assisted wet chemical route and searched their physical and chemical properties. Rilda et al. (2023) have been synthesized with the sol-gel process using mediated *Aspergillus niger* with the four stages of Ti-doped ZnO (Ti/ZnO). The growth and investigation of Ti-doped ZnO nanoparticles subjected to vacuum annealing using solid state reaction by Soniya and Kaleemulla (2023). The basis of the SILAR (Successive Ionic Layer Adsorption and Reaction) method is based on sequential ionic layer adsorption and reaction. In order to avoid homogeneous precipitation on the film, rinsing with deionized water is applied at regular intervals. The originality in this method is the adsorption (deposition) of one substance onto another substance on the substrate. Deposition is achieved by the contact of two different phases. The formation of the film is based on a process resulting from van-der Waals forces or chemical attraction forces that occur between the substrate and the ions in the solution. In this process, factors such as temperature, base feature and surface area, growth rate, pressure and density directly affect the yield. One of the advantages of the SILAR method is enabling the use of temperature-sensitive materials such as insulators, semiconductor metals and polyester. In this way, corrosion and oxidation of the substrate is prevented. Increasing the quality of thin films produced by this method; concentration, solution pH, adsorption, reaction and rinse time parameters. In addition, the thin-film growth technique based on the deposition technique is based on ion-based deposition that occurs in the nucleation regions on the substrate surfaces. The unnecessary of high-quality vacuum and substrate is one of the most important advantages that distinguish the SILAR technique from other expensive techniques. Ade et al. (2021) has reported the doped-ZnO samples produced with SILAR method and the effect of doping on the physical and chemical properties of ZnO samples. In this study, ZnO thin films were grown by the SILAR method with different Ti doping changed from 0.5 % to 0.20 %. The morphological, structural, optical and electrical properties of produced thin films were investigated. In addition, the films with the same additive ratio were annealed at 300 °C for 15 minutes in nitrogen environment. Thus, the effects of both annealing and doping were examined in detail.

2. MATERIAL AND METHOD

2.1. Preparation of Interdigital Electrodes

Initially, glass substrates, for using Ag IDEs, were cut 8 mm wide and 25 mm long. The substrates were cleaned with 20 ml acetone, methanol, and distilled water for 30 min by using an ultrasonic cleaner for each solution, respectively. Substrates dried with dry air were placed on a laser-cut mask with an electrode thickness of 1 mm. Ag metal targets were used to grow IDEs on prepared glass substrates by a thermal evaporation system. Finally, the grown IDEs were annealed at 300 °C in a nitrogen gas environment.

2.2. Preparation of Thin Films

Ti-doped ZnO thin films have been grown by the SILAR method on the glass substrates which the interdigitated Ag electrodes (Ag-IDE) have been evaporated to a side of the substrate. To grow titanium-doped and pure zinc oxide nanostructures, aqueous zinc-ammonia complex ions ($[\text{Zn}(\text{NH}_3)_4]^{2+}$) and aqueous

titanium–ammonia complex ions ($[\text{Ti}(\text{NH}_3)_4]^{2+}$) have been chosen as the cation precursors, in which trace metal basis of ZnCl_2 (99.9%, Sigma-Aldrich) of 0.1 M as a source for Zn, TiO_2 (99%, Merck) of 0.1 M as a source for Ti and aqueous ammonia solution (NH_3 -28%, Sigma-Aldrich) have been used. Deionized water has been used as a solvent. In order to obtain the ($[\text{Zn}(\text{NH}_3)_4]^{2+}$) and ($[\text{Ti}(\text{NH}_3)_4]^{2+}$) complex, ZnCl_2 , TiO_2 , NH_3 and deionized water were mixed in appropriate proportions. All the growth process parameters of nanostructures through the SILAR method are given below, respectively. The glass substrate was kept in the ($[\text{Zn}(\text{NH}_3)_4]^{2+}$) solution for the product undoped ZnO thin film, which was prepared before, for 15 seconds, firstly. The substrate, which was removed from the solution, was kept in distilled water at 80°C during 7s. The substrates, which were in air during 60 s after hot water, were then immersed in distilled water at 25°C and kept there during 30 s. Thus, a cycle is completed (Figure 1). The same process was used to produce titanium-doped thin films. Differently in the production times of undoped ZnO, the glass substrates were kept in the prepared Ti-doped ZnO solution for 20 seconds, while this time was set as 7 seconds for hot water and 40 seconds for pure water at room temperature. This process was completed with forty cycles. After the growth process samples were dried at room temperature for a day. After taking structural, morphological and electrical characterization they annealed at nitrogen environment for 30 minutes. Structural analysis of thin films was evaluated using the Bragg Brentano method by Bruker D8 Advance Twin-Twin X-ray diffractometer (XRD), scanning electron microscope (SEM, FEI Quanta FEG 250), a UV–Vis–NIR spectrophotometer (Jasco V-770 UV-Vis-NIR) and a Keithley 2400 sourcemeter.

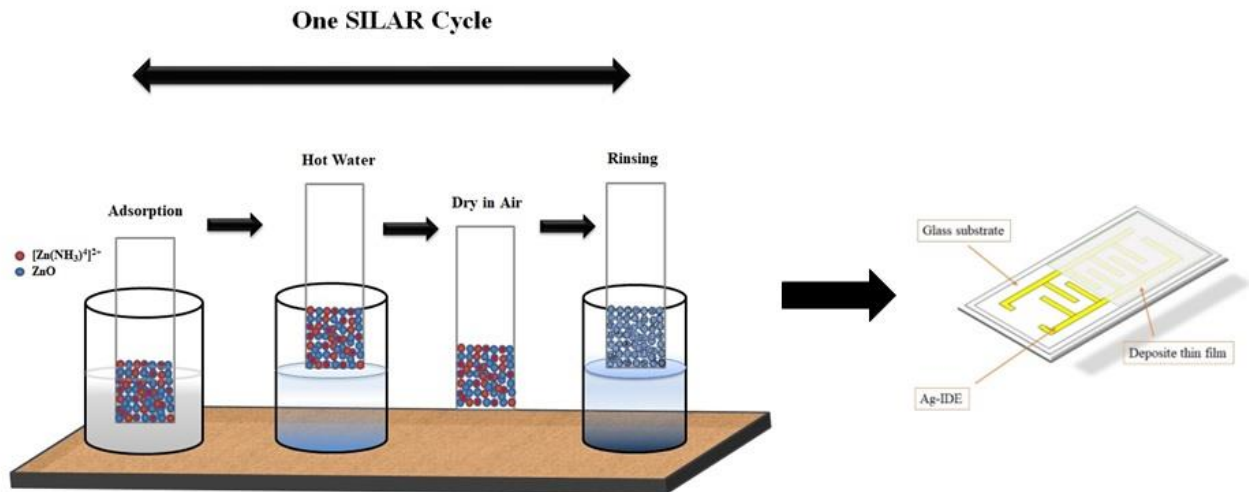


Figure 1. The schematic diagram of SILAR method

3. RESULTS AND DISCUSSION

From Figure 2 to Figure 6 show the SEM images of as-grown and annealed thin films. It was seen that nanorod-like structures were formed as the additive ratio increases in the samples. However, with the $\text{Zn}_{0.85}\text{OTi}_{0.15}\text{O}$ sample, a return to the initial ZnO shape was observed and nanoball-like structures were observed. It was understood that the most suitable doping ratio is 0.10 %. Ti contribution in the $\text{Zn}_{0.90}\text{OTi}_{0.10}\text{O}$ sample. The small-sized nanoball-like particles were seen to be agglomerated, for the pure ZnO thin film. In the SEM images taken from a longer distance, it was seen that the samples were homogeneously distributed and enlarged on the surface. With increasing doping ratio, they have formed as clusters and decrease in the grain size can be observed with increase in annealing temperature. Ade et al. (2021) have grown pure and Ti(1, 3 and 5%)-doped ZnO thin films by the successive ionic layer adsorption and reaction (SILAR) method and an decrease in particle size with doping.

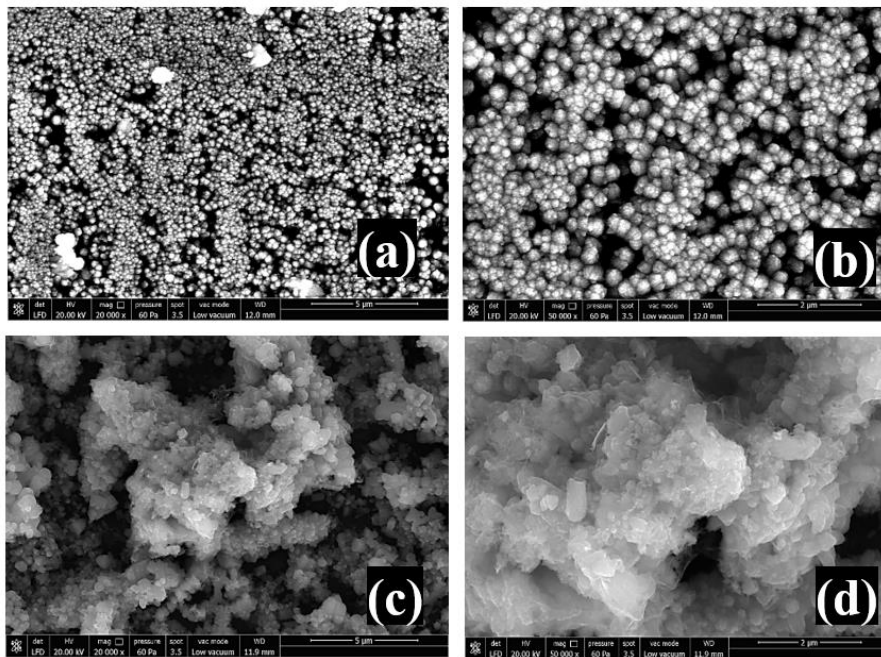


Figure 2. The SEM images of ZnO thin films a), b) as-grown and c), d) heat-treated

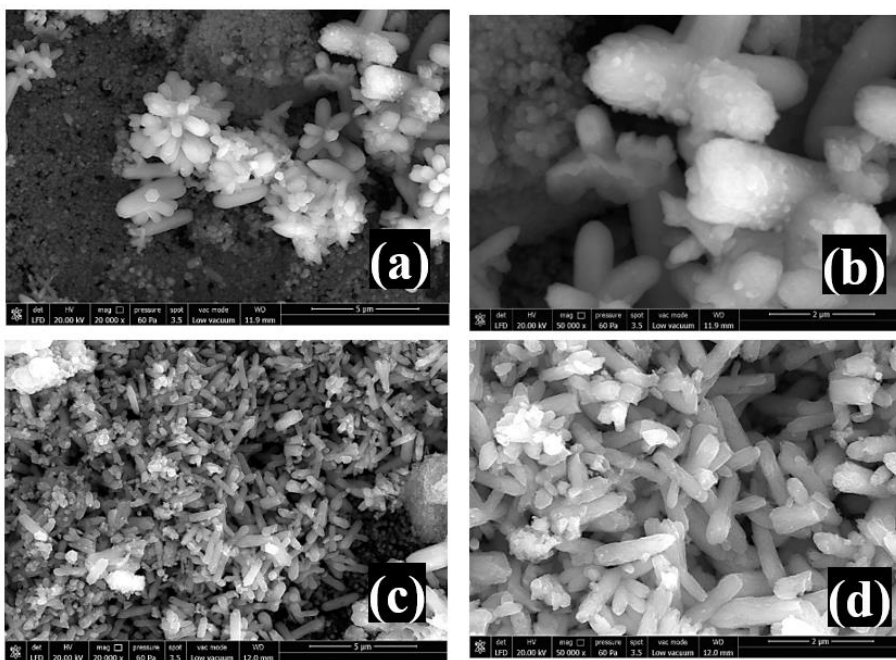


Figure 3. The SEM images of Zn_{0.95}Ti_{0.05}O thin films a), b) as-grown and c), d) annealed

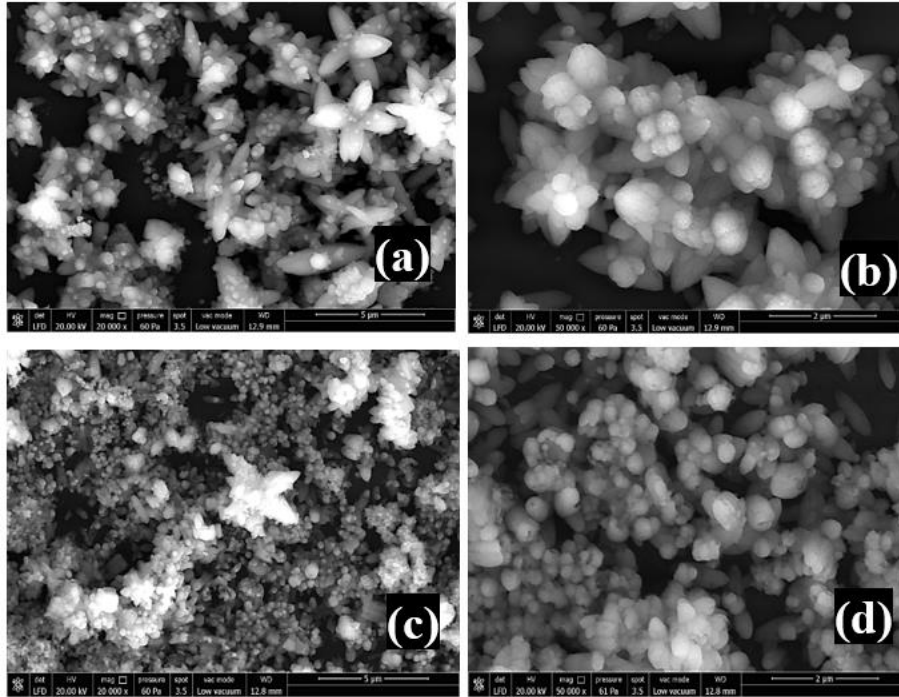


Figure 4. The SEM images of $Zn_{0.90}Ti_{0.10}O$ thin films a), b) as-grown and c), d) annealed

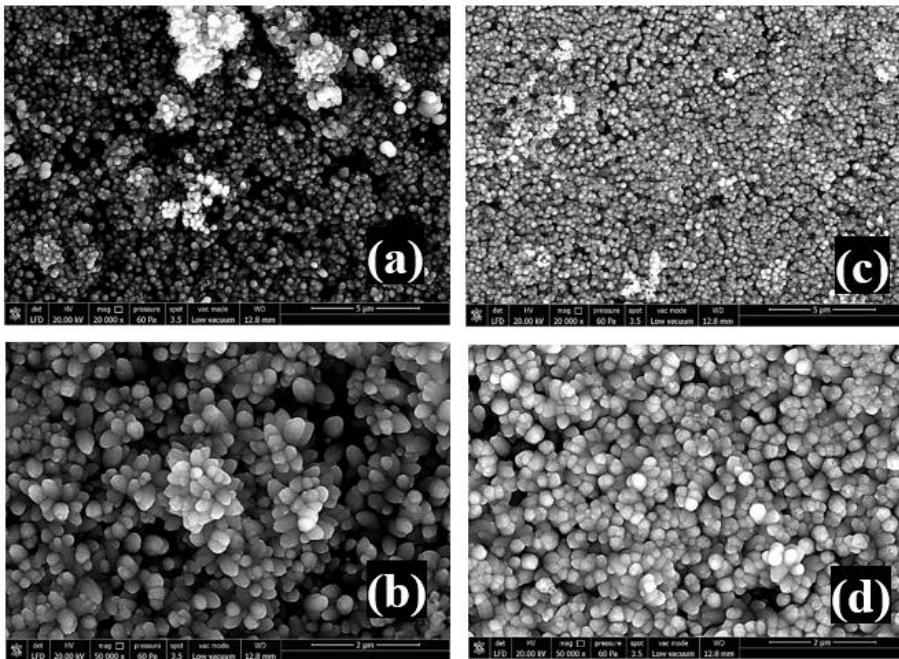


Figure 5. The SEM images of $Zn_{0.85}Ti_{0.15}O$ thin films a), b) as-grown and c), d) annealed

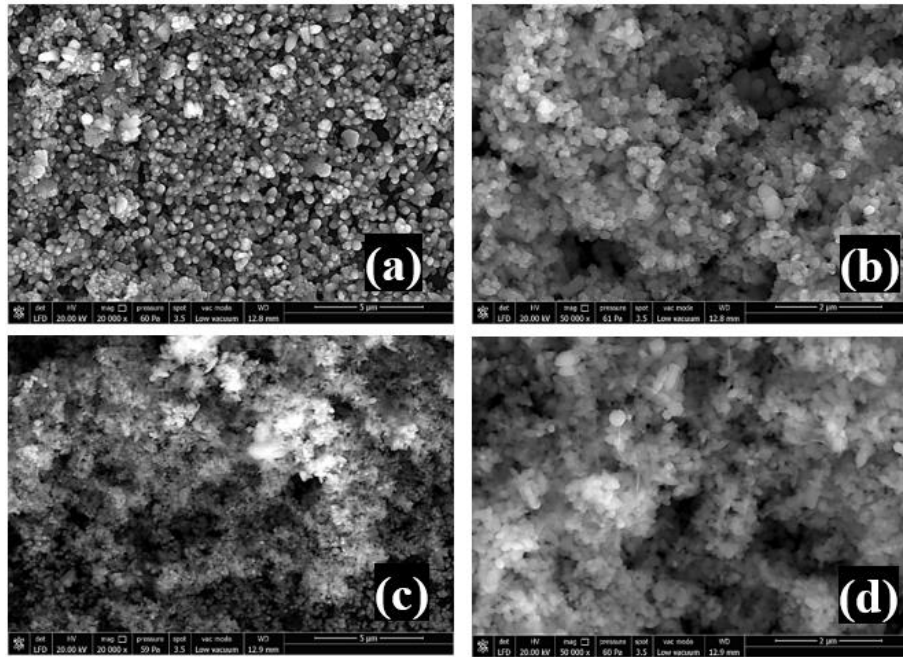


Figure 6. The SEM images of $Zn_{0.80}Ti_{0.20}O$ thin films **a), b)** as-grown and **c), d)** annealed

Figure 7-11 depict the XRD analysis of as-grown and annealed thin films. When the diffraction patterns of the films are examined, the widths and intensities of the peaks differ at each annealing temperature. If the intensities of the peaks in the diffraction patterns are large and the widths are narrow, it means that the crystallization is good in the films, while the intensities of the peaks are small and the widths are large, it means that the crystallization is not good in the films. It was seen that the intensities of the thin films produced are large and the widths are narrow. Crystallization was clearly observed in the produced films. All the films exhibited polycrystalline behavior the PDF 01-071-6424 (Valdés et. al. 2009). Only the peaks belong to the Ti elements which is indexed PDF 00-021-1272 (Li et al., 2014) were seen for $Zn_{0.80}Ti_{0.20}O$ thin film. As the annealing temperature has been implemented, improvements in thin film structures and increases in peak intensities were observed. With the annealing process, the additive atoms settle into the structure and the placed additive atoms increase the crystallization.

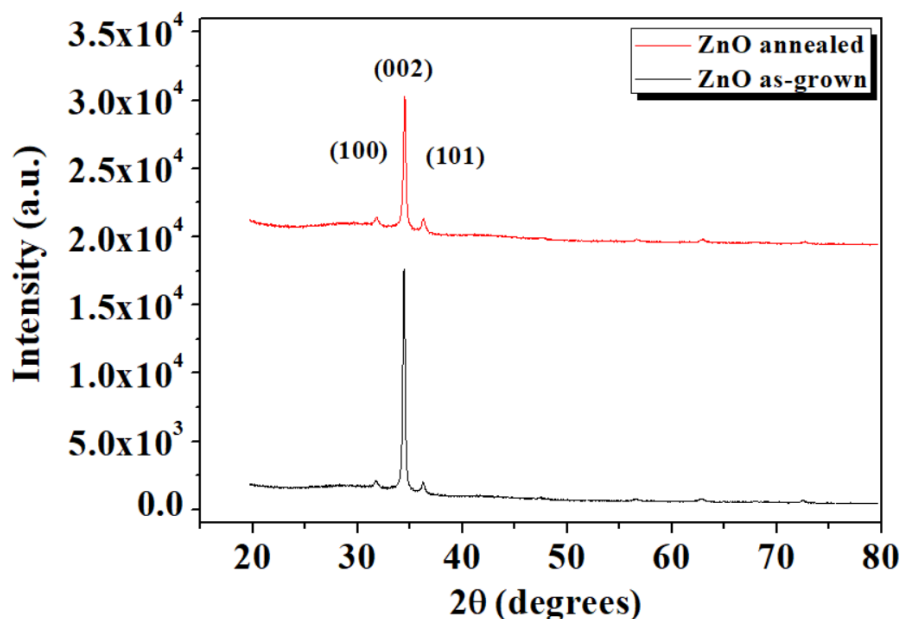


Figure 7. The XRD analyses of ZnO thin films

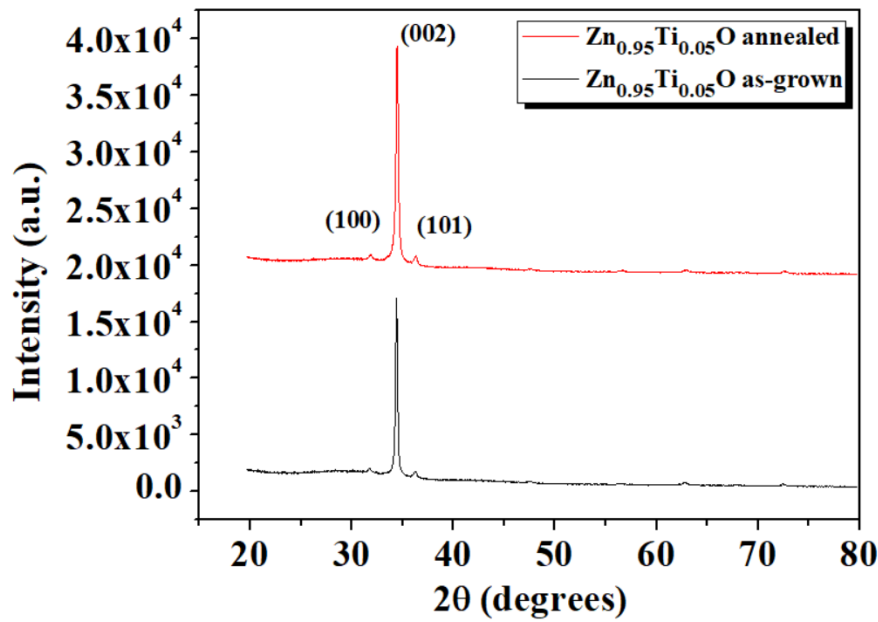


Figure 8. The XRD analyses of $Zn_{0.95}Ti_{0.05}O$ thin films

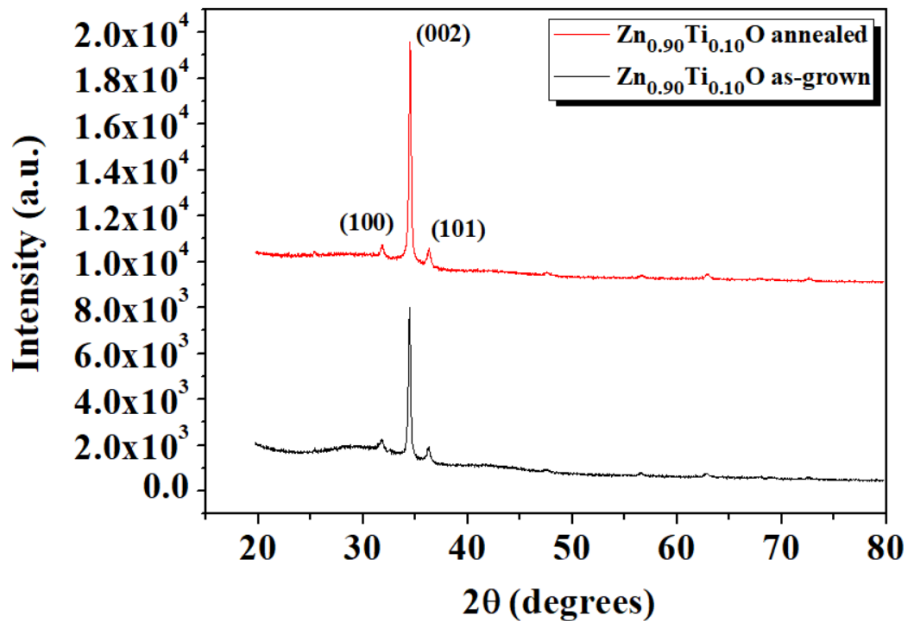


Figure 9. The XRD analyses of $Zn_{0.90}Ti_{0.10}O$ thin films

The crystalline size and dislocation density of produced films are given in Figure 12 and Figure 13. The crystalline for the as-grown samples was calculated as 38.9, 36.8, 36, 34.8 and 34.2 nm for ZnO, $Zn_{0.95}Ti_{0.05}O$, $Zn_{0.90}Ti_{0.10}O$, $Zn_{0.85}Ti_{0.15}O$ and $Zn_{0.80}Ti_{0.20}O$, respectively. The calculations were characterized with Debye-Scherrer's formula (Samuel et al., 2022), and Soniya and Kaleemulla (2023) observed the same results. It may be due to the fact that Ti ions replace Zn ions and do not disrupt the crystal structure. Since the radius of the Ti and Zn ion is 0.68 Å (Ti^{4+}) and 0.74 Å (Zn^{2+}), it can be assumed that the dopant atoms settle in the main unit cell without any deterioration (Soniya & Kaleemulla, 2023). In addition, the crystalline for the annealed samples was calculated as 40, 38.6, 38.2, 37.8 and 37.6 nm for ZnO, $Zn_{0.95}Ti_{0.05}O$, $Zn_{0.90}Ti_{0.10}O$, $Zn_{0.85}Ti_{0.15}O$ and $Zn_{0.80}Ti_{0.20}O$, respectively. The grain size reduction can be mainly attributed to the internal stress increases due to the structural and chemical disorder that causes the system to become unstable when the Ti^{4+} content in the stable ZnO system increases (Soltabayev et al., 2023).

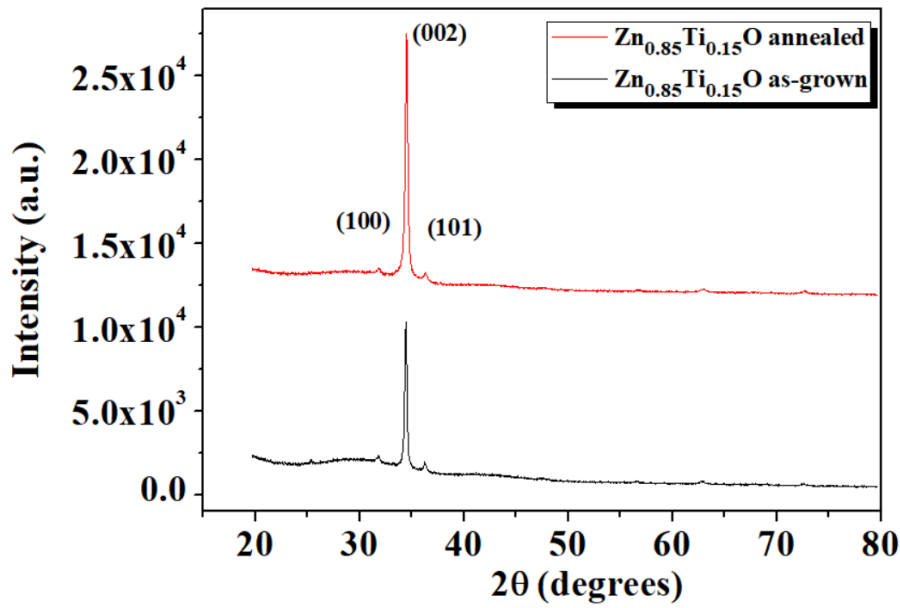


Figure 10. The XRD analyses of $Zn_{0.85}Ti_{0.15}O$ thin films

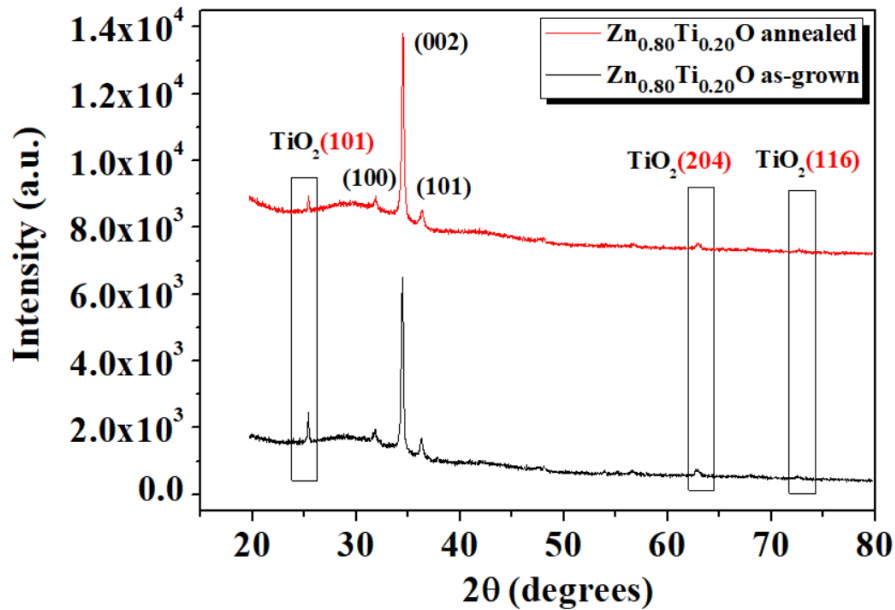


Figure 11. The XRD analyses of $Zn_{0.80}Ti_{0.20}O$ thin films

Figure 14 and Figure 15 present the linear absorbance of as-grown and annealed $Zn_xTi_{1-x}O$ thin films, respectively. The band gap values of as grown samples were calculated 3.35, 3.38, 3.40, 3.39 and 3.38 eV for ZnO , $Zn_{0.95}Ti_{0.05}O$, $Zn_{0.90}Ti_{0.10}O$, $Zn_{0.85}Ti_{0.15}O$ and $Zn_{0.80}Ti_{0.20}O$, respectively. The calculations were made by Tauc Plot (Tekin & Karaduman Er, 2022). Results depended on doping and annealing is in agreement with literature (Pawar et al., 2018). The band gap values in annealed samples were calculated 3.23, 3.28, 3.28, 3.26 and 3.27 eV for ZnO , $Zn_{0.95}Ti_{0.05}O$, $Zn_{0.90}Ti_{0.10}O$, $Zn_{0.85}Ti_{0.15}O$ and $Zn_{0.80}Ti_{0.20}O$, respectively.

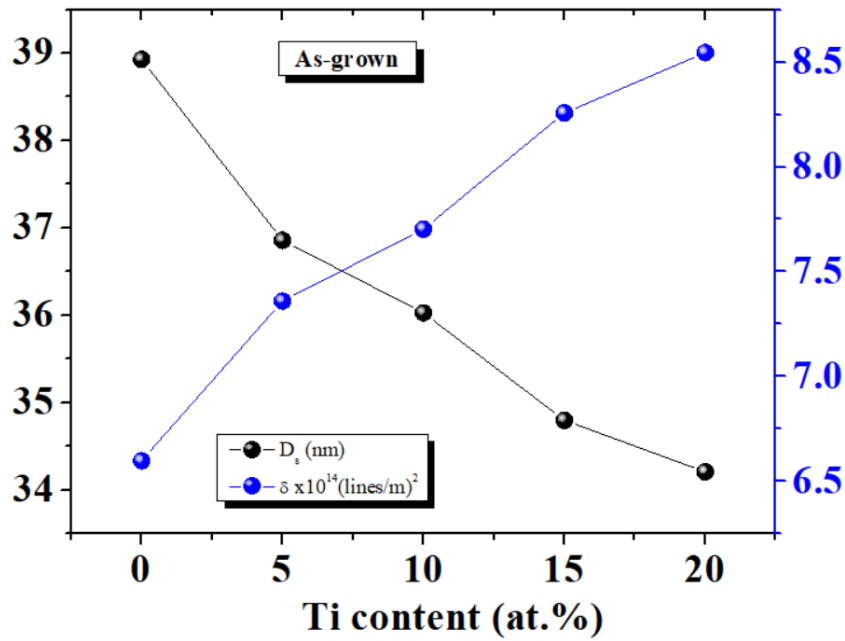


Figure 12. The D and δ of $Zn_xTi_{1-x}O$ thin films; as-grown

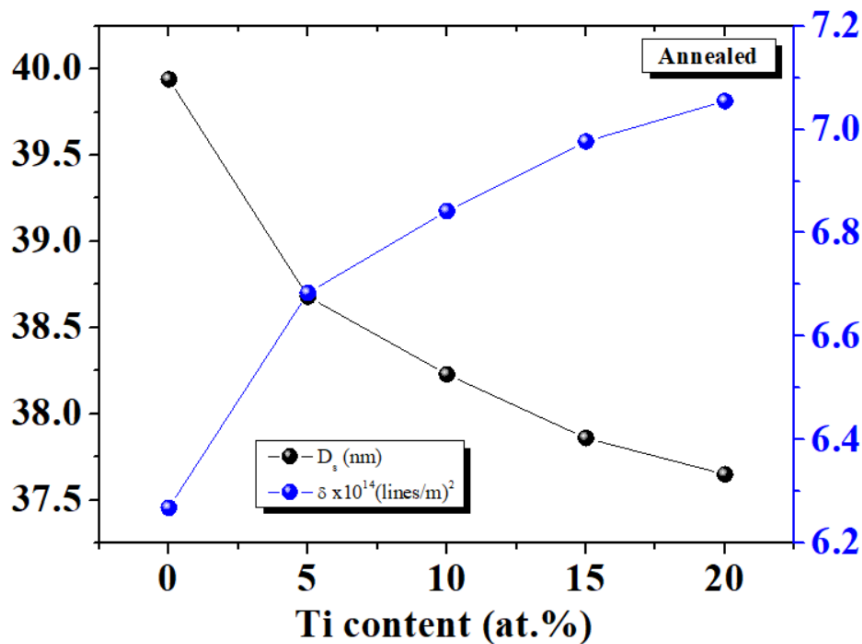


Figure 13. The D and δ of $Zn_xTi_{1-x}O$ thin films; annealed

The I-V graphs of $Zn_xTi_{1-x}O$ thin films are given at Figure 16 and Figure 17. Two probe methods were used for the electrical characterization of the prepared thin films at room temperature. As can be seen from the graph, the samples exhibited the I-V characteristic and Ohmic behavior. The resistance values of as-grown films at 5 V were calculated as 2220, 1779, 1633, 1179 and 956 k Ω for ZnO , $Zn_{0.95}Ti_{0.05}O$, $Zn_{0.90}Ti_{0.10}O$, $Zn_{0.85}Ti_{0.15}O$ and $Zn_{0.80}Ti_{0.20}O$, respectively. If the glass taken directly from the furnace is left to cool at normal temperature, it will crack with the effect of thermal shock, so the annealing process was continued in the furnace and the samples were cooled simultaneously with the cooling of the furnace. The resulting internal stresses were eliminated. Thus, decreases in resistance values were observed with annealing. The resistance values of annealed films were calculated as 907, 734, 678, 485 and 394 k Ω for ZnO , $Zn_{0.95}Ti_{0.05}O$, $Zn_{0.90}Ti_{0.10}O$, $Zn_{0.85}Ti_{0.15}O$ and $Zn_{0.80}Ti_{0.20}O$, respectively (at 5 V).

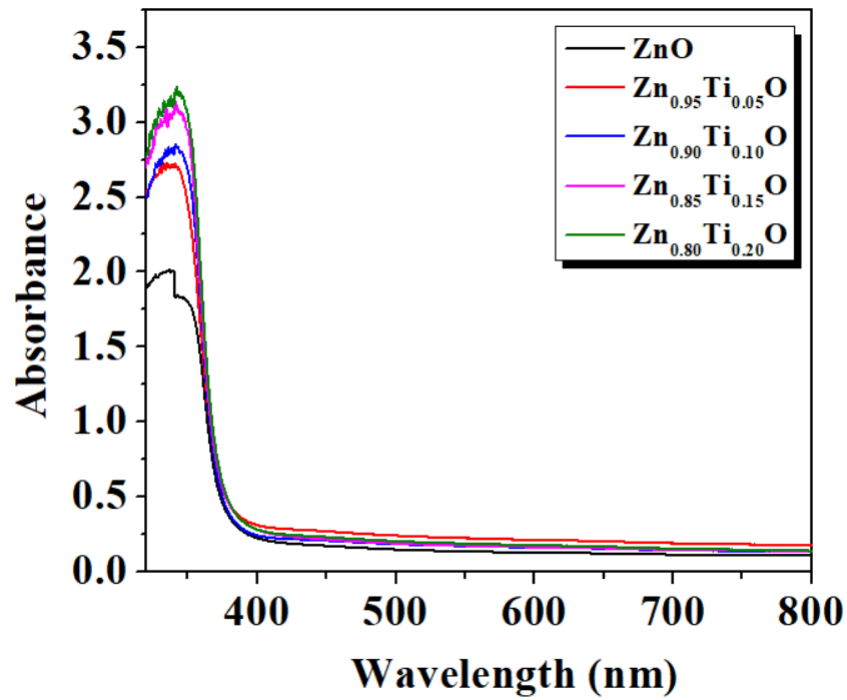


Figure 14. The UV-absorbance analyses of Zn_xTi_{1-x}O thin films

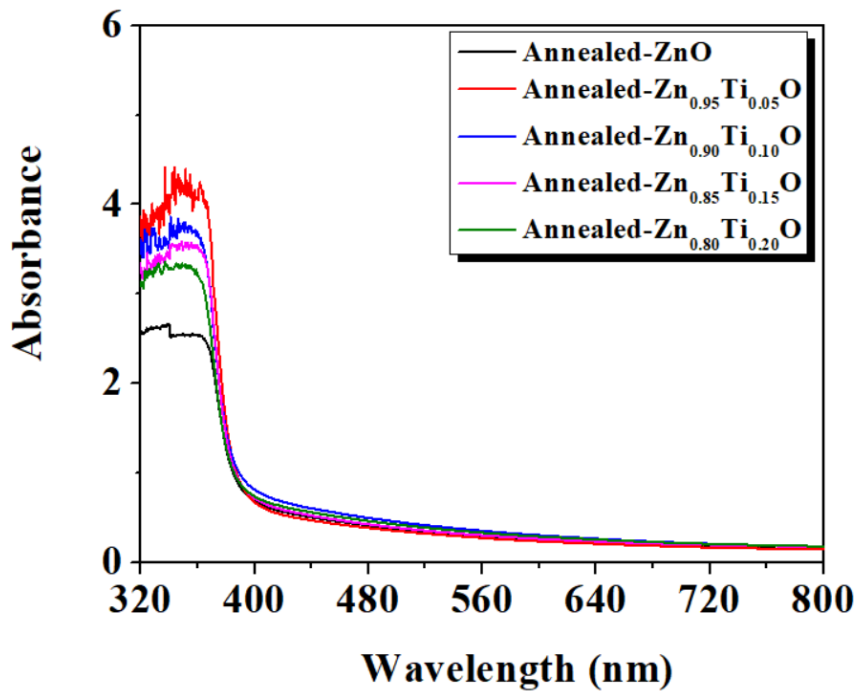


Figure 15. The UV-absorbance analyses of Zn_xTi_{1-x}O thin films

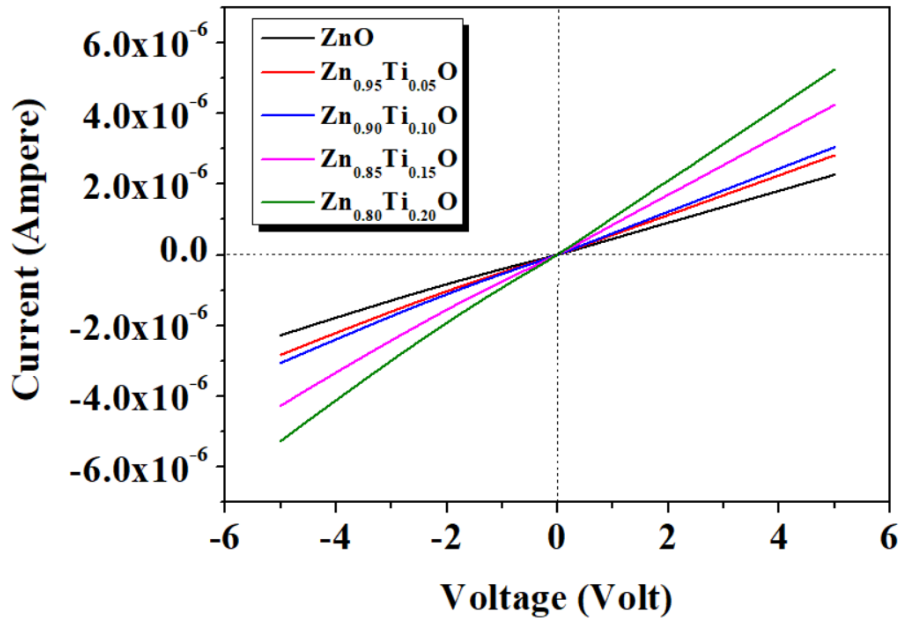


Figure 16. The I-V graphs of $Zn_xTi_{1-x}O$ thin films

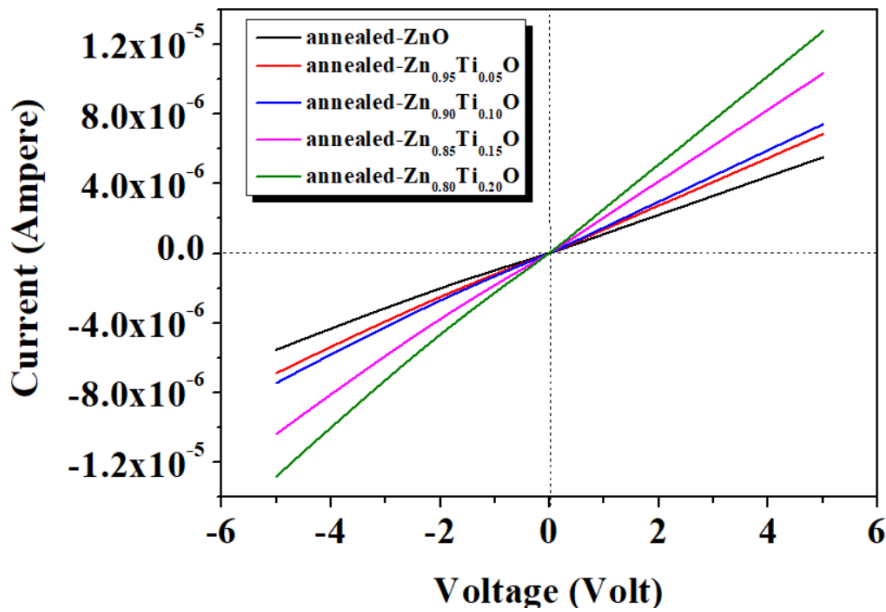


Figure 17. The I-V graphs of $Zn_xTi_{1-x}O$ thin films

4. CONCLUSION

In this study, the variation of structural, electrical and linear absorption properties with both doping rate and annealing was investigated. In the SEM images, it is seen that the samples are homogeneously distributed on the surface and all the films exhibit polycrystalline behavior. The XRD analyzes are showed that the Ti is incorporated into the structure and does not cause deterioration. However, different TiO₂ phases are seen for the Zn_{0.80}Ti_{0.20}O sample. It is seen that there is an increase in the deterioration of the structure of the residual Ti additive. Starting from here, it is thought that 0.15 % contribution is the maximum contribution. This is due to the migration of atoms, which helps incorporation of Ti and oxygen atoms into the lattice regions. As the temperature increased, improvements in thin film structures and increases in peak intensities were observed. As can be seen from the graph, the samples exhibit the I-V characteristic and Ohmic behavior.

ACKNOWLEDGEMENT

Gazi University Scientific Research Fund financially supports this study with project code: FDK-2023-8722].

CONFLICT OF INTEREST

The authors declare no conflict of interest.

REFERENCES

- Ade, R., Kumar, S. S., Valanarasu, S., Kumar, S. S., Sasikumar, S., Ganesh, V., Bitla, Y., Algarni, H., & Yahia, I. S. (2021). Enhanced optoelectronic properties of Ti-doped ZnO nanorods for photodetector applications. *Ceramics International*, 47(17), 24031-24038. doi:[10.1016/j.ceramint.2021.05.112](https://doi.org/10.1016/j.ceramint.2021.05.112)
- Darmadi, I., Taufik, A., & Saleh, R. (2020). Analysis of optical and structural properties of Ti_doped ZnO nanoparticles synthesized by co-precipitation method. *Journal of Physics: Conference Series*, 1442(1), 012021. doi:[10.1088/1742-6596/1442/1/012021](https://doi.org/10.1088/1742-6596/1442/1/012021)
- Hsu, S.-F., Weng, M.-H., Chou, J.-H., Fang, C.-H., & Yang R.-Y. (2016). Effect on the Ti-target arc current on the properties of Ti-doped ZnO thin films prepared by dual-target cathodic arc plasma deposition. *Ceramics International*, 42(13), 14438-14442. doi:[10.1016/j.ceramint.2016.06.043](https://doi.org/10.1016/j.ceramint.2016.06.043)
- Lee, M. L., Wang, J. C., Kao, C. H., Chen, H., Lin, C. Y., Chang, C. W., Mahanty, R. K., Lin, C. F., & Chang, K. M. (2018). Comparison of ZnO and Ti-doped ZnO sensing membrane applied in electrolyte-insulator-semiconductor structure. *Ceramics International*, 44(6), 6081-6088. doi:[10.1016/j.ceramint.2017.12.239](https://doi.org/10.1016/j.ceramint.2017.12.239)
- Li, W., Liang, R., Hu, A., Huang, Z., & Zhou, Y. N. (2014). Generation of oxygen vacancies in visible light activated one-dimensional iodine TiO₂ photocatalysts. *RSC Advances*, 4(70), 36959-36966. doi:[10.1039/C4RA04768K](https://doi.org/10.1039/C4RA04768K)
- Pawar, S. T., Chavan, G. T., Prakshale, V. M., Jadkar, S. R., Kamble, S. S., Maldar, N. N., & Deshmukh, L. P. (2018). Probing into the optical and electrical properties of hybrid Zn_{1-x}Co_xSe thin films. *Journal of Materials Science: Materials in Electronics*, 29(5), 3704-3714. doi:[10.1007/s10854-017-8302-7](https://doi.org/10.1007/s10854-017-8302-7)
- Rilda, Y., Valeri, A., Syukri, S., Agustien, A., Pardi, H., & Sofyan, N. (2023). Biosynthesis, characterization, and antibacterial activity of Ti-doped ZnO (Ti/ZnO) using mediated *Aspergillus niger*. *South African Journal of Chemical Engineering*, 45, 10-19. doi:[10.1016/j.sajce.2023.04.001](https://doi.org/10.1016/j.sajce.2023.04.001)
- Samuel, J., Suresh, S., Shabna, S., Sherlin Vinita, V., Joslin Ananth, N., Shajin Shinu, P. M., Mariappan, A., simon, T., Samson, Y., & Biju, C. S. (2022). Characterization and antibacterial activity of Ti doped ZnO nanorods prepared by hydrazine assisted wet chemical route. *Physica E: Low-dimensional Systems and Nanostructures*, 143, 115374. doi:[10.1016/j.physe.2022.115374](https://doi.org/10.1016/j.physe.2022.115374)
- Shewale, P. S., & Yu, Y. S. (2016). H₂S gas sensing properties of undoped and Ti doped ZnO thin films deposited by chemical spray pyrolysis. *Journal of Alloys and Compounds*, 684, 428-437. doi:[10.1016/j.jallcom.2016.05.178](https://doi.org/10.1016/j.jallcom.2016.05.178)
- Soltabayev, B., Ajjaj, A., Yergaliuly, G., Kadyrov, Y., Turlybekuly, A., Acar, S., & Mentbayeva, A. (2023). Ultrasensitive nitric oxide gas sensors based on Ti-doped ZnO nanofilms prepared by RF magnetron sputtering system. *Journal of Alloys and Compounds*, 953, 170125. doi:[10.1016/j.jallcom.2023.170125](https://doi.org/10.1016/j.jallcom.2023.170125)
- Soniya, P. G., & Kaleemulla, S. (2023), Properties of Ti doped ZnO nanoparticles under solid state reaction method involving vacuum annealing. *Physica B: Condensed Matter*, 649, 414409. doi:[10.1016/j.physb.2022.414409](https://doi.org/10.1016/j.physb.2022.414409)
- Tekin, S., & Karaduman Er, I. (2022). The structural, morphological, optical and gas-sensing properties of Mn₃O₄ thin films grown by successive ionic layer adsorption and reaction technique. *Journal of Materials Science: Materials in Electronics*, 33(18), 14519-14534. doi:[10.1007/s10854-022-08372-w](https://doi.org/10.1007/s10854-022-08372-w)